Response of the Equatorial Ionosphere to the Geomagnetic *DP*2 current system

E. Yizengaw[1], M. B. Moldwin[2], E. Zesta[3], M. Magoun[1], R. Pradipta[1], C. M. Biouele[4], A. B. Rabiu[5], O. K. Obrou[6], Z. Bamba[7], and E. R. de Paula[8]

[1]Institute for Scientific Research, Boston College, Boston, USA; [2]Department of Climate, Space Sciences and Engineering, University of Michigan, Ann Arbor, USA; [3]NASA Goddard Space Flight Center, Greenbelt, Maryland, USA; [4]Department of Physics, University of Yaoundé I, Yaoundé, Cameroon; [5]National Space Research and Development Agency, Abuja, Nigeria; [6]Laboratorie de physique de l'atmosphère, Université Félix Houphouët-Boigny FHB, Abidjan, Cote d'Ivoire. [7]Centre de Recherche Scientifique de Conakry Rogbanè, Conakry, Guinea; [8]Instituto Nacional de Pesquisas Espaciais (INPE), São José dos Campos, Brazil

Abstract: The response of equatorial ionosphere to the magnetospheric origin *DP*2 current system fluctuations is examined using ground-based multi-instrument observations. The interaction between the solar wind and magnetosphere generates a convection electric field that can penetrate to the ionosphere and cause the *DP*2 current system. The quasi-periodic *DP*2 current system, which fluctuates coherently with fluctuations of the IMF Bz, penetrates nearly instantaneously to the dayside equatorial region at all longitudes and modulates the electrodynamics that governs the equatorial density distributions. In this paper, using magnetometers at high and equatorial latitudes, we demonstrate that the quasi-periodic *DP*2 current system penetrates to the equator and causes the dayside equatorial electrojet (*EEJ*) and the independently measured ionospheric drift velocity to fluctuate coherently with the high-latitude *DP*2 current as well as with the *IMF Bz* component. At the same time, radar observations show that the ionospheric density layers move up and down, causing the density to fluctuate up and down coherently with the *EEJ* and *IMF Bz*.

This is the author manuscript accepted for publication and has undergone full peer review but has not been through the copyediting, typesetting, pagination and proofreading process, which may lead to differences between this version and the Version of Record. Please cite this article as doi: 10.1002/2016GL070090

Introduction

It is well known that geomagnetic disturbances in the high-latitude region consist of two morphologically distinct current systems (*DP*1 and *DP*2 currents) that are associated directly with magnetospheric convection. The *DP*1 (disturbance polar of the first type) current (the substorm westward electrojet) disturbance, which is associated with the substorm expansion phase [*Claver and Kamide,* 1985], is characterized by a strong intensification of the westward auroral electrojet and cause the formation of magnetic bays in the auroral region [*Nishida, 1968*]. While the *DP1* current system is localized in the near local midnight region, the polar region *DP*2 (disturbance polar of the second type) current disturbances is global and characterized by quasi-periodic magnetic fluctuations with a timescale of 30 minutes to several hours [*e.g., Nishida,* 1968; *Kikuchi et al.,* 1996; 2000; 2008]. Unlike the *DP*1 current system, the *DP*2 current system can occur during both quiet and disturbed times and its impact can be detected at all latitudes with different magnitudes [*Claver and Kamide,* 1985]. All of these phenomenological characteristics have been determined primarily from ground magnetometer observations over many decades.

Understanding the formation of the quasi-periodic ionospheric current systems is very important to our comprehension of the solar wind magnetosphere-ionosphere coupling process and its impact on the equatorial density distribution. In the presence of interplanetary magnetic field, the interaction between solar wind and magnetosphere produces a dawn-to-dusk convection electric field ($E_y = -(V_x \times B_z)$). This electric field can then penetrate into the magnetosphere when the *IMF Bz* turns south, and drives *DP2* current system [*Nishida,* 1968]. The equivalent *DP2* current fluctuation, which consists of twin current vortices at high latitudes and zonal current component at low latitudes, then extends all over the Earth from the pole to the equator and [*e.g., Nishida,* 1968]. Since the solar wind speed is relatively steady compared to *IMF Bz*, the time fluctuation of the convection electric field may be directly proportional to the variation of *IMF Bz* instead of solar wind speed. Thus, the time fluctuation of the *DP*2 current systems both at high-latitude and equatorial region is primarily controlled by the *IMF Bz* fluctuation. *Nishida,* [1968], using the combined data from Explorer 18 (IMP 1) spacecraft and ground-based magnetometers, demonstrated that the *DP*2 currents both at high and equatorial latitudes coherently fluctuate with *IMF Bz*. Therefore, the presence of the *DP*2 current fluctuation at the equator is the direct result of the quasi-periodic interplanetary electric field that penetrates into the magnetosphere and down to the equatorial ionosphere through the TM0 (zero order transverse magnetic) mode waves in the Earth-ionosphere waveguide *Kikuchi et al.* [2008].

When the *IMF Bz* turns south the interaction between the geomagnetic field and *IMF* produces two reconnection locations, at the dayside (sunward side) and nightside (tail side) [*Nishida, 1968*]. Although it is the source of many important processes, such as energization of charged particles and expansion of substorm (or formation of *DP*1 current system), the field-aligned currents that originate from nightside reconnection may not be the cause for the *DP*2 current system; because the transit time of the event from the tail side reconnection region (away from the ground by 10s to few hundred R_E) to the ground is much greater than the *DP*2 fluctuation time. This implies that field-aligned currents that originate from dayside reconnection drives the *DP*2 current system. However, the time varying interplanetary electric field can penetrate into the magnetosphere if the electric conductivity along the field lines on the magnetopause is low. *Parker* [1967] suggested the magnetopause surface conductivity decreases in the region where the angle between solar wind velocity and the geomagnetic field decrease. Since the conductivity along the field lines on front side of the magnetopause is believed to be high, the time varying electric field cannot penetrate to the magnetosphere from the front side of the magnetopause but instead it penetrates from around the morning-evening sector of the magnetopause where field-aligned electric conductivity is low and the finite potential difference is applied across the magnetopause [*Nishida, 1968*].

Although there have been many studies of the *DP2* current system and its impact on magnetic fluctuations in the equatorial region [*e.g.*, Nishida, 1967; *Clauer and Kamide*, 1985; *Kikuchi et al.*, 1996; 2000; 2008; *Trivedi et al.*, 2002], there are still several important questions that remain unresolved. One of these major questions is; what kind of impact can the *DP*2 current system impose on the equatorial ionospheric density distribution? This study for the first time shows the response of the ionospheric density distribution to the fluctuation of the *DP*2 current system at the equator, that can modulate the equatorial electrodynamics to fluctuate with the same periodicity as the *DP*2 current system or as *IMF Bz*.

Data Analysis

For this study, we used data from ground-based magnetometers that are located at auroral and equatorial latitudes to estimate the *DP*2 currents and the *EEJ* that occurred on 16 February 2016 and 2 May 2010. The detailed description of the technique that we use to identify the *DP*2 current systems and *EEJ* from the magnetometer observations can be found in [*e.g., Kikuchi et al.,* 1996] and [*Anderson et al.,* 2004; *Yizengaw et al.,* 2014, and the reference therein], respectively. The magnetometers we use for this study are operated under the umbrella of African Meridian *B*-field Education and Research (AMBER) [*Yizengaw and Moldwin,* 2009], INTERMAGNET [*Love and Chulliat,* 2003], and the Low Latitude Ionospheric Sensor Network (LISN) [*Valladares and Chau,* 2012] projects. The geographic and geomagnetic coordinates of the magnetometers used are listed in *Table 1*.

Similarly, to estimate the response of the ionosphere to the *DP*2 current system dynamics, we use vertical total electron content (*VTEC*) measurements from GPS receivers operated under the LISN networks and ionosonde observations from the Global Ionospheric Radio Observatory (GIRO) network [*Reinisch and Galkin,* 2011]. Figure 1 shows the location of all magnetometers, GPS receivers, and ionosonde stations that are used in this study. The solid and dashed curves depict the location of the magnetic equator and the region of EEJ (i.e., ±3.5° magnetic latitudes), respectively. The colored solid curves at the bottom left corner of Figure 1 shows the ground tracks of the GPS satellites, of which the PRN and the starting time of each pass are also shown at the beginning of each pass.

Observations:

Figure 2 (top panel) shows the characteristics of solar wind parameters; *IMF Bz* (black curve) and the dawn-to-dusk interplanetary electric field (*IEF*) (red curve) observed on 16 February 2016. Both of them show strong quasi-periodic fluctuations with a dominant periodicity of around 45 minutes. Although the solar wind parameters show periodic fluctuations, there was no significant magnetic storm activity. *Dst* index was quiet with $Dst > -60\ nT$ but *Kp* index indicates the presence of a moderate storm with $Kp = 5$, which is surprising as the *DP2* current fluctuation can also occur during geomagnetically quiet periods [*Claver and Kamide*, 1985].

The second panel from the top in Figure 2 depicts the X-components (approximately north-south direction) magnetic field variations obtained from four magnetometers located at high and auroral latitudes. Different colors represent different stations where the stations' codes and geomagnetic latitudes are shown at the right side. In order to maintain the magnetic field fluctuation within the same range limit, we multiplied the magnetic field fluctuation with the correspondingly colored numbers shown inside each panel.

The third panel of Figure 2 from the top, indicates the X-component magnetic field fluctuations observed in the equatorial region, within $\pm 8^{\circ}$ geomagnetic latitude, using stations located at different longitudes. The different colors represent different longitudes (noted on the right side of the panel), expanding from west American to west African regions. All of them exhibit coherent fluctuation with *IMF Bz*, in which the fluctuations are stronger around local noon when solar UV irradiation is stronger and thus ionosphereic conductance enhanced. Finally, the *EEJ*, which is directly proportional to the equatorial vertical drift [*e.g., Anderson et* al., 2004] that governs the equatorial ionospheric density distribution, that was calculated at two different longitudes show identical fluctuation (see the bottom panel of Figure 2) with the same periodicity of *IMF Bz* fluctuations. The magnitude and direction of *EEJ* is calculated using pairs of ground magnetometers located approximately at the dip equator and off the geomagnetic equator (~6–9° geomagnetic) latitudes [*Anderson et al.*, 2004; *Yizengaw et al.*, 2014]. The vertical solid lines, shown from second to bottom panels, depict the local noon for the corresponding stations. The vertical dashed lines shown in all panels indicate the time coincidence of the *IMF Bz* minimum point (or the *IEF* peaks), the magnetic variation peaks at different latitudes and longitudes, and the *EEJ* peaks.

Figure 3 presents the response of the ionosphere for the quasi-periodic fluctuations of the solar wind parameters and the *EEJ* measurements. The top panel shows the *EEJ* at the western and eastern side of South America, which is the same as in Figure 2 bottom panel. The vertical solid lines indicate the local noon for the correspondingly colored *EEJs*. The second panel from the top show the *VTEC* obtained by the GPS receiver located at Jicamarca on 16 February 2016. The corresponding filtered *VTEC* (by subtracting the sixth order polynomial fit from the actual *VTEC*) shows clear *VTEC* fluctuations that exhibit good correlation with *EEJ* fluctuation. Different colors represent the *VTEC* segment obtained by tracking different GPS satellites in which the pseudo-random noise (PRN) numbers of each satellite are given at the right side. The ground tracks of each satellite are shown, as line curves, in Figure 1, which are correspondingly colored as the *VTEC* curves shown in the second and third panels of Figure 3. The contour in the bottom two panels in Figure 3 depicts the aggregate number of return echoes recorded by the digisonde at Boa Vista on 15 and 16 February 2016 (as a function of height and time). Ionograms were recorded once every 15 minutes, and the return echoes are summed over all sounding frequencies. The color represents the level of total echo amplitudes at any given height and time, and the white curve indicates the *EEJ* estimated from the nearby pair of magnetometers located at the *76.9°W* meridian. The height of maximum total echo amplitude often coincides with hmF2, especially in terms of their time rate of change. Thus, we used the height of maximum total echo amplitude fluctuations to track the up-and-down movement of the ionospheric F-layer, which is a good indicator how the ionospheric density fluctuates up and down in the presence of *DP2* current systems.

The top panel in Figure 4 shows another example, specifically the periodic *IMF Bz* (black curve) fluctuations and the respective *IEF* (red curve) observed on 2 May 2010. The middle panel presents the magnetic variation observed at three equatorial stations located at different longitudes which are noted on the right side, and the fluctuations are stronger around local noon. The solid vertical lines depict local noon of the corresponding stations. Unlike the 16 February 2016 event, the Jicamarca radar was running on JULIA (Jicamarca Unattended Long-term investigations of the Ionosphere and Atmosphere) mode and provided ionospheric vertical irregularity drifts during the 2 May 2010 event. The irregularity vertical drift (red curve) is overplotted with the *EEJ* (black curve) estimated using the pair of ground magnetometers in the Jicamarca meridian and is shown in the bottom panel of Figure 4. The irregularity drift shows excellent correlation with the *EEJ* and with the *IMF Bz* quasi-periodic fluctuations shown in the top panel, implying a source and effect relationship between the *IMF* fluctuations and the vertical drift fluctuations at the equator.

Discussion and Conclusion

The interaction between the solar wind and the magnetosphere drives the region 1 (*R1*) and region 2 (*R2*) field aligned current (*FAC*) systems and the associated magnetospheric plasma convection. The *R1* & *R2* *FAC*s in general setup electric field that may generate current system at high latitude that has quasi-periodic fluctuation with very good one-to-one correlation with the *IMF Bz* variations. Since the magnetic effect of Pederson currents on the ground level is roughly equal in magnitude but opposite in sign to the magnetic effect of FAC, the magnetic disturbance observed at high-latitudes ground level is due to Hall currents [*e.g., McPherron,* 1995]. Thus, the *DP2* fluctuations at high-latitudes are due to the combined effect of Hall conductivity and the solar wind-driven convection electric field [*e.g., Clauer and Kamide,* 1985; *Kikuchi et al.*, 1996; 2000]. The *DP2* fluctuation then extends to the equatorial ionosphere almost instantaneously (see Figures 2 & 4) through the TM0 mode waves in the Earth-ionosphere waveguide [*e.g., Kikuchi et al.*, 2008].

The second panel in Figure 2 shows the magnetic field at northern high and auroral latitudes (THL, IQA, and NAQ) that mostly do not show clear correlation with *IMF Bz* fluctuations during the given time interval (09:00 UT – 20:00 UT). The polar region (THL) magnetic variation was experiencing a deep magnetic bay during this time interval, which is expected as the station was in the nightside during February. The strong magnetic bays were also observed at auroral latitudes (IQA) during 9-14 UT, which was in local morning toward local noon indicated by the blue vertical solid line. After 14:00 UT (i.e., when the station was moving to dayside) the *DP*2 current dominates at IQA and shows coherent fluctuations with *IMF Bz* during 14:00-17:00UT. The magnetic field variations at NAQ, of which its local noon is located at ~15:00UT as indicated by green solid vertical line, do not show any significant magnetic bay; instead it shows good correlation with *IMF Bz* during 14:00-19:00 UT. The mid-latitude station (KEP) located on the dayside southern region mostly shows one-to-one correlation with the *IMF Bz* fluctuations. The comparison of magnetic fluctuations at different latitudes, such as at THL, IQA, NAQ, KEP, shows the *DP2* fluctuations indeed decrease in magnitude as latitude decreases until it gets enhanced considerably (see the third panel from the top of Figure 2) due to the presence of Cowling effect at the dip equator.

The question is - what makes the *DP2* current system fluctuates both at high and low-latitudes coherently? It has been demonstrated that this could be due to the imbalance of *R1* and *R2 FAC* current systems. By separating the *R1* and *R2 FAC*s from radar electric field measurements, using the combination of ground-based magnetometers and EISCAT radar data, *Kikuchi et al.* [2000] showed a significant decrease (increase) of *EEJ* at the geomagnetic equator when *IMF Bz* turns north (south) and when there is a steep decrease (increase) of *R1 FAC*s and increase (decrease) of *R2 FAC*s. The *R2 FAC*s generally setup a transient electric field that is opposite in direction with that of *R1 FAC*s and produce a shielding effect [*e.g., Kikuchi et al.,* 2008].

Similarly, when *IMF Bz* turns south (north) both the *DP*2 current system and the *EEJ* at the equator gets enhanced (decayed) or becomes eastward (westward), and irregularity drift at the equator turns upward (downward) as shown in Figure 2 & 3. The excellent time coincidence between the *IMF Bz* minimum points and *EEJ* peaks, as pointed out by the vertical dashed lines that pass through them, indicates that the *EEJ* enhanced (decayed) when *IMF Bz* turns south (north) which is consistent with the results reported in *Kikuchi et al*. [2000].

Thus, comparing Figures 2 and 3 the vertical dashed lines provide an excellent view that the periodic imbalance of *R1* & *R2 FACs* systems causes the *EEJ* and thus the vertical drift velocity fluctuation at the equator. The fluctuating vertical drift, which controls the vertical motion of the ionosphere, in turn causes the F-layer vertical height to fluctuate up (down) coherently with *IMF Bz* as shown in Figure 3. The positions of *EEJ* peaks (white curves) are directly correlated with ionosonde estimated ionospheric backscatter echo peaks as shown in the fourth panel from the top of Figure 3. The fluctuating height of backscatter echo amplitude peaks, which often coincides with hmF2, is used to track the up-and-down movement of the ionospheric F-layer. While the strong F-region echoes show clearly visible up and down fluctuations of the F-layer's virtual height during *DP*2 fluctuations event on 16 February, the echoes detected by the same ionosonde during the time without *DP*2 fluctuations event on 15 February do not show any up and down fluctuation. This clearly demonstrates how the *DP2* current fluctuation controls not only the electrodynamics but also the ionospheric F-layer height. Similarly, the filtered *VTEC* from four different satellites (third panel in Figure 2) show almost coherent fluctuation with the

EEJ and thus with *IMF Bz*. The time delay between the filtered *VTEC* as well as the ionospheric echo and *EEJ* peaks, in which the *VTEC* and ionospheric echo peaks appears about 20-30 minutes after *EEJ* peak time, is due to the duration of the vertical drift perturbation and that the ionospheric density peaks occur at the time when the layer stops moving upward or when the drift velocity reverse its direction. This clearly demonstrates that the magnetospheric origin quasi-periodic electric field can penetrate to the magnetosphere and drive *DP*2 current fluctuations that extend to the lower latitude ionosphere and causes the *EEJ* and thus vertical drift at the equator to fluctuate and create significant effect on the equatorial density distribution by making the F-layer moves up and down. The bottom panel of Figure 4 shows another example of the *DP2* current modulation of the drift velocity as it is demonstrated by the independently measured ionospheric irregularity drift (red curve) that fluctuates coherently with the *EEJ* as well as with *DP*2 current and *IMF Bz*. Similar correlation between the magnetospheric origin electric field and the ground-based radar measured electric field during magnetic storm periods have been performed, mainly in the absence of *DP2* current fluctuation [*e.g., Kelley et al.*, 2003; *Huang et al.*, 2007; *Sobral et al.*, 1997]. However, for the first time, we report the solar wind-magnetosphere-ionosphere interactions driven *DP2* current systems not only modulate ionospheric equatorial electrodynamics but also cause the ionospheric density distributions to fluctuate up and down.

It is worth mentioning about the small-scale fluctuation embedded in the large quasi-periodic *EEJ* variation, *e.g.*, shown in between 16:45 – 17:50 UT in Figure 4. *Yizengaw et al.* [2013]

reported that the *ULF* wave in the *Pc5* range is the possible cause for the formation of those small-scale *EEJ* fluctuations that are predominantly visible in Figure 4 compared to that of Figure 2 where these fluctuations are visible only at the eastward peaks of *EEJ*.

In general, when the *FAC*s are in continuous dynamic, they form significantly fluctuating *DP*2 current systems that can easily penetrate to the equatorial region and modulate the equatorial electrodynamics that are responsible for the complicated nature of dayside ionospheric density height variations at the equator. Therefore, understanding of the *DP*2 current systems, such as its source, condition of its penetration to the equatorial region, and the impact it can produce onto the ionospheric density distribution is very important to understand the physics of equatorial electrodynamics that govern the equatorial density distribution. Because its impact on the equatorial ionosphere is significant, it can greatly affect the communication and navigation systems.

Acknowledgment

This work has been partially supported by AFOSR (FA9550-12-1-0437 and FA9550-15-1-0399) and NSF (AGS145136, AGS1450512) grants. The authors are indebted to the Jicamarca radio observatory (JRO) and INTERMAGNET team for the magnetometer data resources they made available to the public. We also thank the global ionospheric radio observatory team for the ionosonde data. The solar wind data were obtained from the CDAWeb database.

References

Anderson, D., A. Anghel, J. Chau, and O. Veliz (2004), Daytime vertical E × B drift velocities inferred from ground-based magnetometer observations at low latitudes, *Space Weather*, *2*, S11001, doi:10.1029/2004SW000095.

Basu, S., Su. Basu, F. J. Rich, K. M. Groves, E. MacKenzie, C. Coker, Y. Sahai, P. R. Fagundes, and F. Becker-Guedes (2007), Response of the equatorial ionosphere at dusk to penetration electric fields during intense magnetic storms, *J. Geophys. Res., 112, A08308*, doi:10.1029/2006JA012192.

Clauer, C. R., and Y. Kamide (1985), *DP*l and *DP*2 current systems for the March 22, 1979 substorms, *J. Geophys. Res., 90,* 1343-1354, 1985.

Huang, C.-S., S. Sazykin, J. L. Chau, N. Maruyama, and M. C. Kelley (2007), Penetration electric fields: Efficiency and characteristic time scale, *J. Atmos. Sol. Terr. Phys.*, doi:10.1016/j.jastp.2006.08.06.

Kelley, M. C., J. J. Makela, J. L. Chau, and M. J. Nicolls (2003), Penetration of the solar wind electric field into the magnetosphere/ionosphere system, *Geophys. Res. Lett. 30 (4), 1158*, doi:10.1029/2002GL016321.

Kikuchi, T., H. Lu¨hr, T. Kitamura, O. Saka, and K. Schlegel (1996), Direct penetration of the polar electric field to the equator during a DP2 event as detected by the auroral and equatorial magnetometer chains and the EISCAT radar, *J. Geophys. Res., 101(A8), 17161– 17173.*

Kikuchi, T., H. Lühr, K. Schlegel, H. Tachihara, M. Shinohara, *and* T.-I. Kitamura (2000), Penetration of auroral electric fields to the equator during a substorm, *J. Geophys. Res.*, *105*, *23,251–23,261*, doi:10.1029/2000JA900016.

Kikuchi, T., K. K. Hashimoto, and K. Nozaki (2008), Penetration of magnetospheric electric fields to the equator during a geomagnetic storm, *J. Geophys. Res., 113, A06214*, doi:10.1029/2007JA012628.

Love, J. J. and A. Chulliat (2003), An International Network of Magnetic Observatories, *Eos*, *94(42), 373-374*.

McPherron, R. L. (1995), Magnetospheric dynamics, *in Introduction to Space Physics, edited by M. G. Kivelson and C. T. Russell, pp.400-458, Cambridge Univ. Press, New York,*

Nishida, A. (1968), Coherence of geomagnetic DP2 magnetic fluctuations with interplanetary magnetic variations, *J. Geophys. Res., 73(17), 5549–5559*.

Parker, E. N. (1967), Small-scale nonequilibrium of the magnetopause and its consequences, *J. Geophys. Res., 72(17), 4365–4374.*

Sobral, J. H. A., M. A. Abdu, W. D. Gonzalez, B. T. Tsurutani, I. S. Batista, and A. L. C. Gonzalez (1997), Effects of intense storms and substorms on the equatorial ionosphere/thermosphere system in the American sector from ground-based and satellite data, *J. Geophys. Res., 102(A7), 14,305–14,313*.

Trivedi, N. B., D. G. Sibeck, E. Zesta, J. C. Santos, K. Yumoto, T. Kitamura, M. Shinohara, *and* S. L. G. Dutra (2002), Signatures of traveling convection vortices in ground magnetograms under the equatorial electrojet, *J. Geophys. Res., 107, 1087,* doi:10.1029/2001JA000153.

Valladares, C. E., *and* J. L. Chau *(*2012*),* The Low-Latitude Ionosphere Sensor Network: Initial results, *Radio Sci*., 47*, RS0L17, doi:10.1029/2011RS004978*

Yizengaw, E., and M. B. Moldwin (2009), African Meridian B-field Education and Research (AMBER) Array, *Earth Moon Planet,104(1), 237-246,* doi:10.1007/s11038-008-9287-2.

Yizengaw, E., E. Zesta, C. M. Biouele, M. B. Moldwin, A. Boudouridis, B. Damtie, A. Mebrahtu, F. Anad, R. F. Pfaff, and M. Hartinger (2013), Observations of ULF wave related equatorial electrojet fluctuations, *J. Atmos. Solar-Terr. Phys., 103, 157-168.*

Yizengaw, E., M. B. Moldwin, E. Zesta, C. M. Biouele, B. Damtie, A. Mebrahtu, B. Rabiu, C. E. Valladares, and R. Stoneback (2014), The longitudinal variability of equatorial electrojet and vertical drift velocity in the African and American sectors, *Ann. Geophys., 32, 231–238.*

Table 1: List of instruments used for this study

Stations	Geographic Coordinate		Geomagnetic Coordinate		Operated under the umbrella of
	Latitude (°N)	Longitude (°E)	Latitude (°N)	Longitude (°E)	
List of Magnetometers					
Abidjan	4.60	-6.64	-6.0	65.82	AMBER
Abuja	10.5	7.55	-0.55	79.63	AMBER
Belem	-1.45	-48.5	-1.05	25.34	AMBER
Conakry	10.5	-13.71	-0.46	60.37	AMBER
Petrolina	-9.5	-40.5	-6.95	30.21	AMBER
Yaounde	3.78	11.52	-5.30	83.12	AMBER
Jicamarca	-11.95	-76.88	0.61	-5.40	JICAMARCA
Piura	-5.17	-80.64	6.84	-9.40	JICAMARCA
Alta Floresta	-9.87	-56.1	-0.75	15.18	LISN
Cuiaba	-15.56	-56.1	-5.85	13.80	LISN
Leticia	-4.2	-69.9	8.18	2.00	LISN
Huancayo	-12.05	-75.33	0.63	-3.89	INTERMAGNET
Iqaluit	63.75	-68.52	73.21	14.91	INTERMAGNET
King Edward Point	-54.28	-36.49	-43.64	24.75	INTERMAGNET
Mbour	14.38	-16.97	2.06	58.24	INTERMAGNET
Narsarsuaq	61.16	-45.44	66.47	43.91	INTERMAGNET
Port Stanley	-51.70	-57.89	-37.63	10.55	INTERMAGNET
Qaanaaq (Thule)	77.47	-69.23	85.63	33.34	INTERMAGNET
GPS receivers					
Jicamarca	-11.95	-76.88	-0.87	16.35	LISN
Ionosonde Station					
Boa Vista	2.8	-60.7	12.55	13.47	GIRO

Figure Caption:

Figure 1: The geographic locations of the ground-based instruments that are used in this analysis.

Figure 2. (top to bottom) *IMF Bz* (black curve) and *IEF* (red curve), the X-component of four high latitudes magnetometers, X-component magnetic field variation from six equatorial magnetometers, and *EEJ* estimated at different meridians.

Figure 3. *EEJ* estimated at two different longitudes (top panel), *VTEC* segments from four different *PRN* and the corresponding filtered *VTEC* (second and third panels from the top). The bottom two panels show the range-time-intensity-style plot of ionospheric echoes received from ionosonde located at Boa Vista, and the over-plotted white curves depict the *EEJ* during the corresponding days given at the top of each panel.

Figure 4. As for Figure 2 but for a different day that is given at the top of the panels.

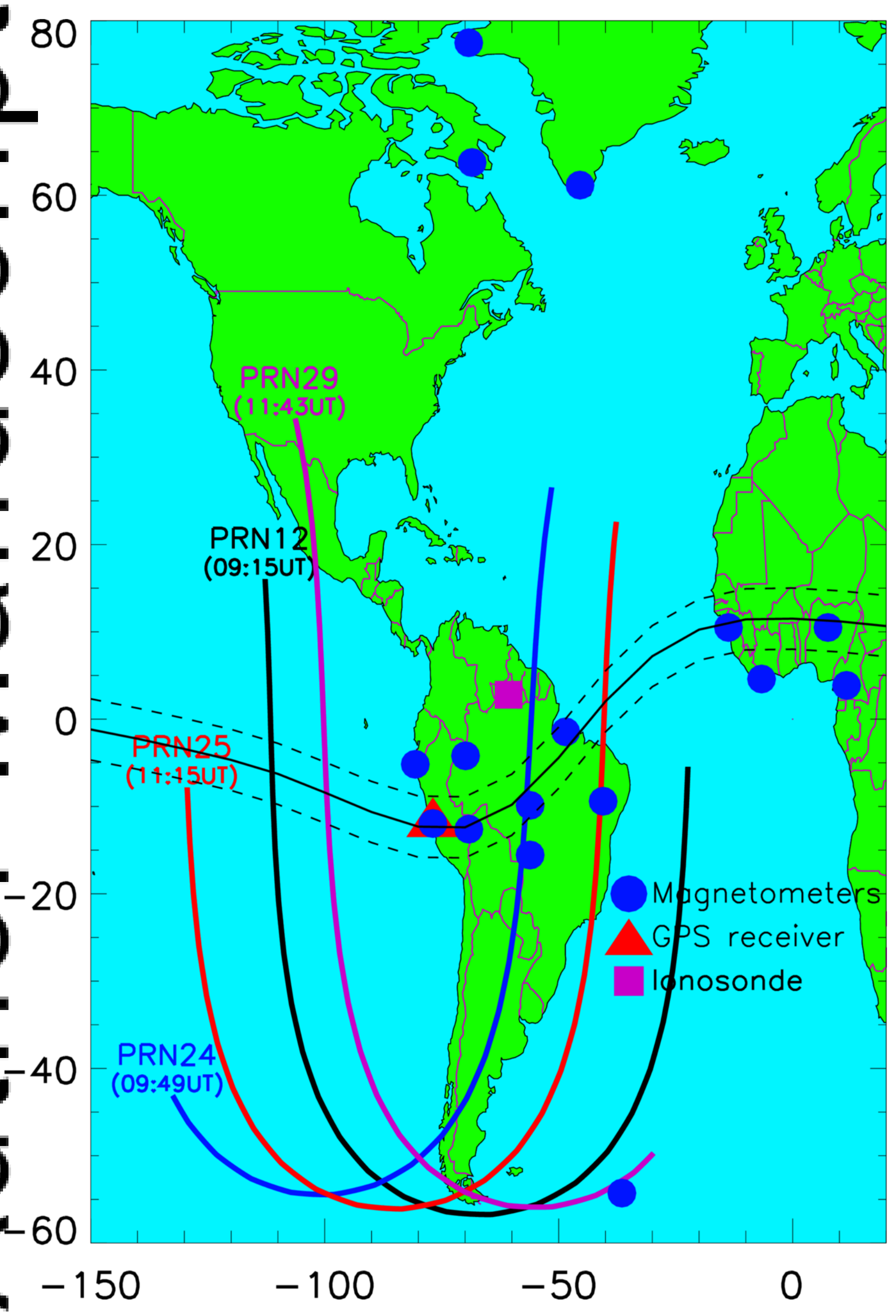

2016gl070090-f01-z-.eps

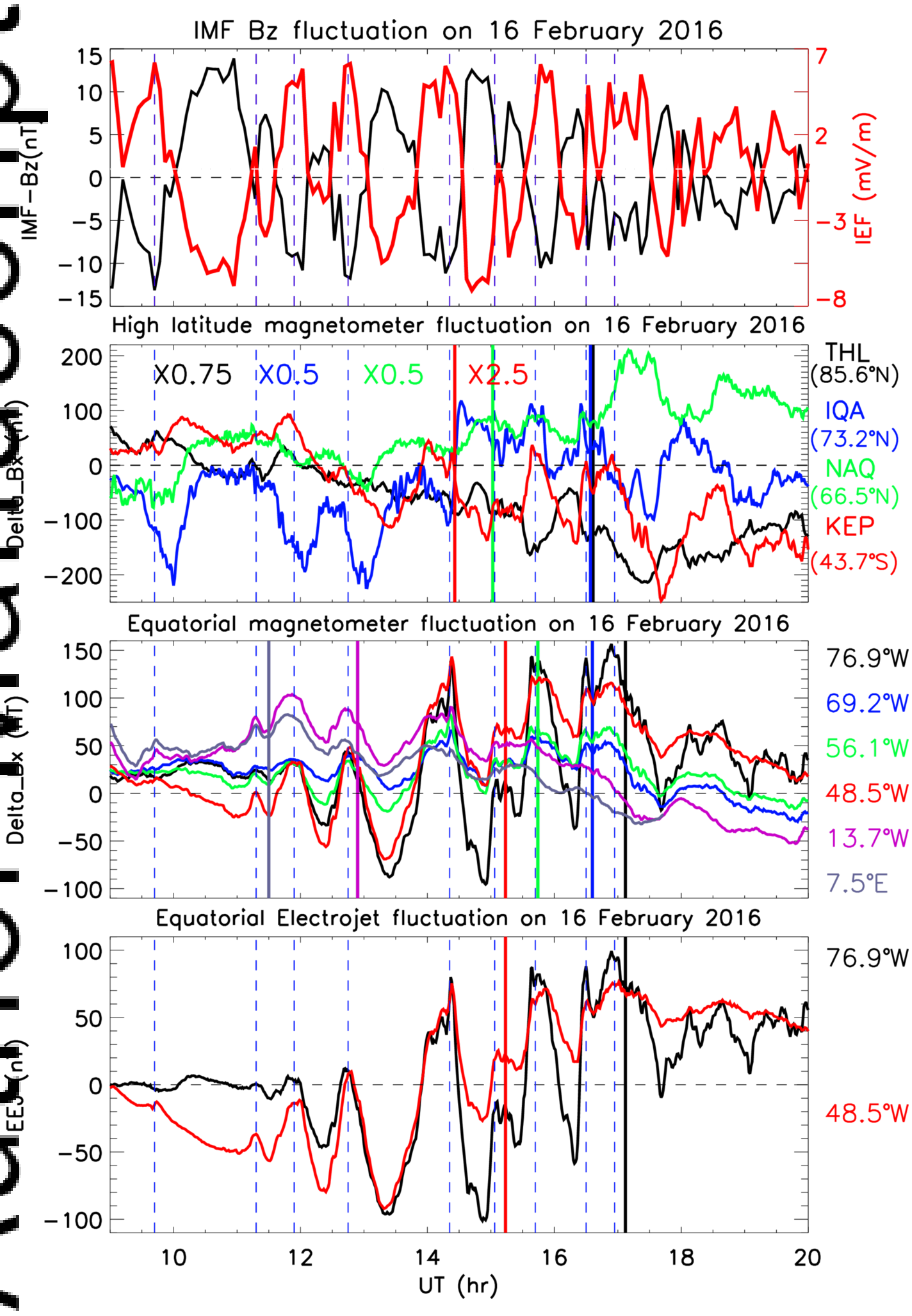

2016gl070090-f02-z-.eps

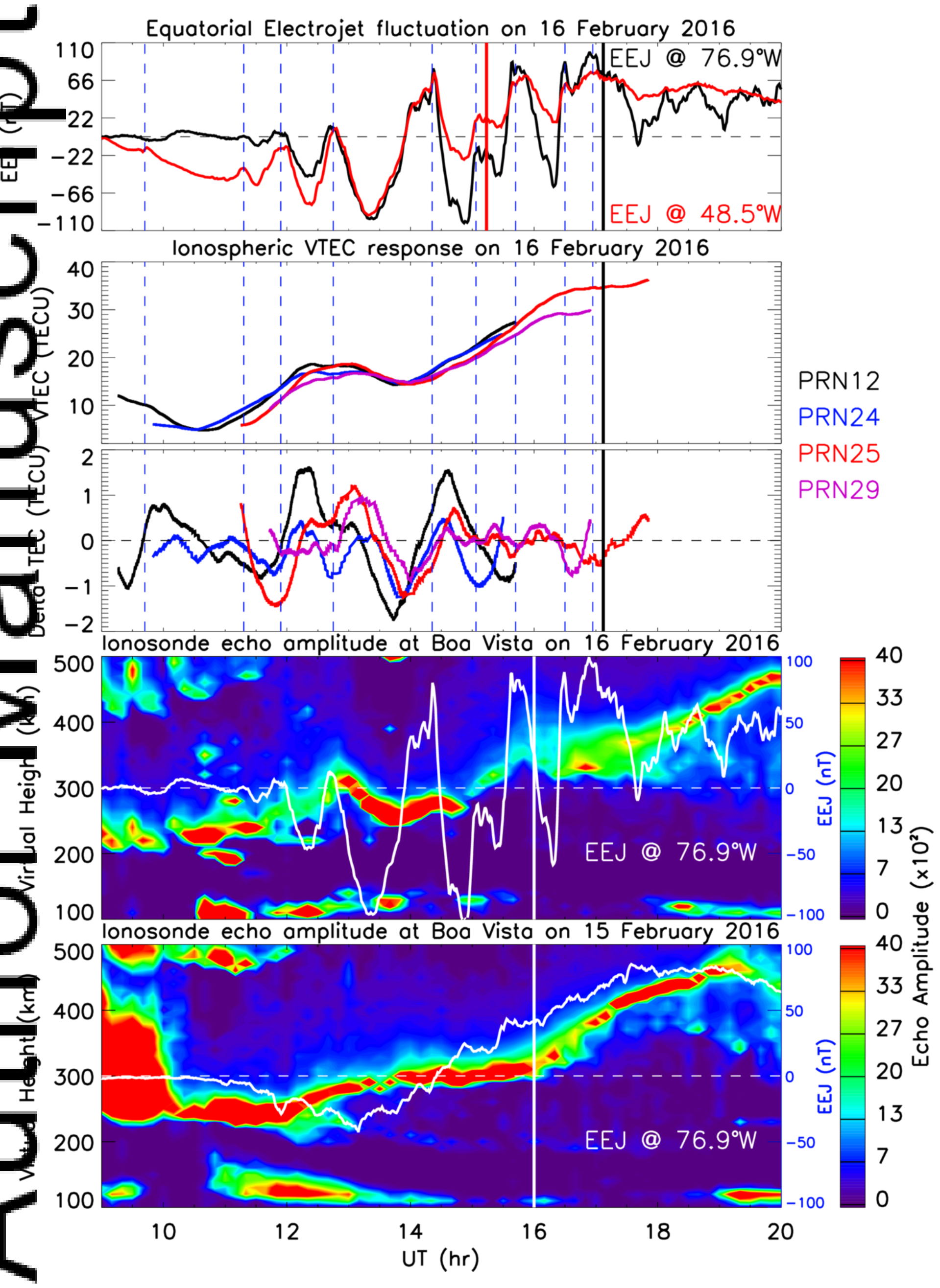

2016gl070090-f03-z-.eps

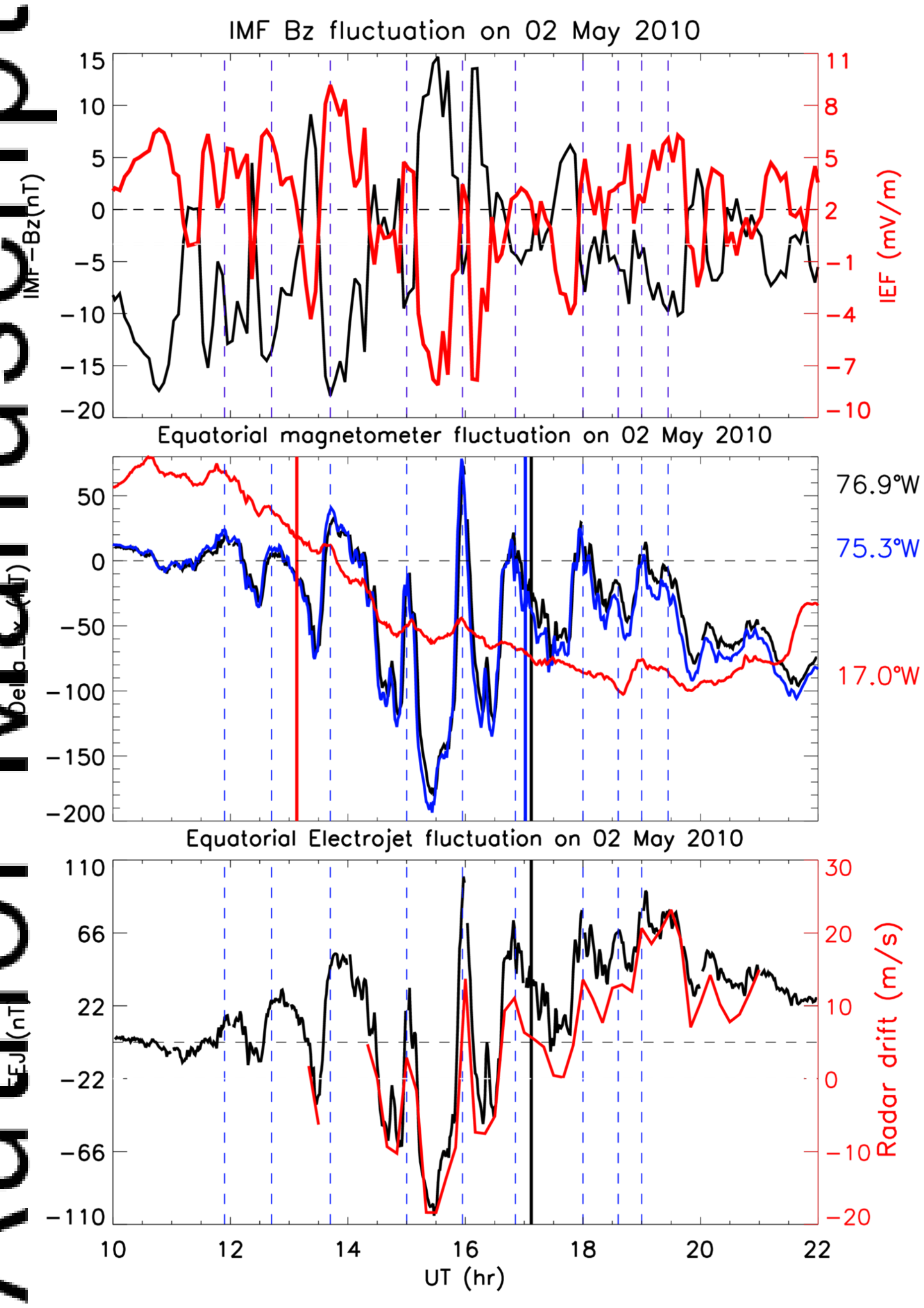

2016gl070090-f04-z-.eps